# Scattering of atoms by a corrugated potential wall of finite height

J. R. Manson*
*Department of Physics and Astronomy, Clemson University, Clemson, South Carolina 29631*

G. Armand
*Centre d'Études Nucléaires de Saclay, Service de Physique Atomique, Section d'Études des Interactions Gaz-Solides, B.P. 2, 91190 Gif-sur-Yvette, France*

(Received 9 July 1979)

We consider the quantum-mechanical problem of the scattering of a particle by a corrugated wall potential of finite height, and the results are applied to the diffraction of low-energy atoms by a crystalline surface. Two approximate solutions are discussed and both are based on the idea of taking the known form of the wave function deep inside the surface and extending it up into the selvedge region. Comparison with similar calculations for a corrugated hard wall shows that the effect of allowing penetration of the wave function into the surface is not qualitatively different, but variations of the order of 10–20% in certain diffracted intensities can be readily obtained.

## I. INTRODUCTION

There have recently been a number of calculations reported for the diffraction of low-energy neutral atoms by a solid surface using the corrugated-hard-wall (CHW) model.[1-4] In this model the interaction potential between particle and surface is zero if $z > \phi(\vec{R})$ and infinite if $z < \phi(\vec{R})$, where $\vec{R}$ is the position vector parallel to the surface, $z$ is the perpendicular position vector, and $\phi(\vec{R})$ is a periodic function giving the corrguation of the surface. Some of these calculations have given very good agreement with experimental data under widely different surface conditions, particularly when the effects of an attractive well near the surface are included.[5,6] However, because of its simplicity, the CHW model is open to a number of criticisms, one of the most important being that the wave function is forced to vanish inside the surface. In reality, the repulsive part of the interaction potential should have a finite height, and perhaps more importantly a finite slope which would permit penetration of the wave function into the solid. In this work we choose to model the penetration of the wave function by considering a corrugated wall potential of finite height in order to see the influence of a possible wave penetration on the diffracted peak intensities. The exact solution of this problem is substantially more complicated than the CHW model so we have considered two different approximate solutions. Both of these approximations have exponentially decaying behavior deep inside the surface and the approximation consists in assuming that these forms of the wave function can be extended into the selvedge region.

We begin in Sec. II with a brief review of the CHW problem which forms the basis of the formalism for the finite height (or soft-wall) potential presented in Sec. II. In Sec. IV we apply the formalism to the specific case of a triangular surface profile, and calculations are presented for both approximate solutions and compared to the available experimental data.

## II. THE CORRUGATED-HARD-WALL PROBLEM

A convenient starting point for the elastic CHW problem is the integral equation for the Schrödinger wave function $\psi_i$ which can be written as[3]

$$\psi_i = \phi_i + \sum_l \phi_l \frac{1}{E_i - E_l + i\epsilon} T_{li} , \tag{1}$$

where $\phi_l$ is a plane-wave state with corresponding eigenvalue $E_l$, and the transition matrix $T_{fi}$ is given by

$$T_{fi} = \int d\vec{r}\, \phi_f^* V \psi_i . \tag{2}$$

The infinite potential at the surface gives rise to a $\delta$-function singularity in the second derivative of the wave function which, in turn, must be reflected in the product $V\psi_i$:

$$V(\vec{r})\psi_i(\vec{r}) = f(\vec{R})\delta(z - \phi(\vec{R}))\exp(i\vec{K}_i \cdot \vec{R}) . \tag{3}$$

The function $f(\vec{R})$ is the source function or emitting function and must be determined by application of appropriate boundary conditions to Eq. (1). As a result of condition (3) and the periodicity of the surface many of the integrals in Eq. (1) become trivial and one can readily obtain the following form for the wave function, valid for all $z$:

$$\psi(\vec{r}) = e^{i\vec{K}_i \cdot \vec{R}} e^{ik_{iz}z} - \sum_{\vec{G}} \frac{e^{i(\vec{K}_i + \vec{G}) \cdot \vec{R}}}{k_{Gz}} \times \int_{uc} d\vec{R}' F(\vec{R}') e^{-i\vec{G} \cdot \vec{R}'} e^{ik_{Gz}|z - \phi(\vec{R}')|} , \tag{4}$$

 © 1979 The American Physical Society

where the incident wave vector has components $\vec{K}_i$ and $k_{iz}$ parallel and perpendicular to the surface, respectively; $F(\vec{R}) = (im/\hbar^2 a) f(\vec{R})$ with $m$ the mass of the particle and $a$ the area of the surface unit cell; $\vec{G}$ is a surface reciprocal lattice vector; and $k_{Gz} = [K_i^2 + k_{iz}^2 - (\vec{K}_i + \vec{G})^2]^{1/2}$. The integral is carried out over a single unit cell of the surface. It is clear that in the asymptotic region $z > \phi_{\max}$ the wave function consists of the incoming beam plus outgoing diffracted beams with coefficients

$$C_{\vec{G}} = \frac{1}{k_{Gz}} \int_{uc} d\vec{R} F(\vec{R}) e^{-i\vec{G}\cdot\vec{R}} e^{-ik_{Gz}\phi(\vec{R})} . \tag{5}$$

The experimentally measured intensity of each diffracted beam is then

$$I_G = \frac{k_{Gz}}{k_{iz}} |C_{\vec{G}}|^2 . \tag{6}$$

The appropriate boundary condition for the CHW problem in order to determine $F(\vec{R})$ is that the wave function must vanish on the surface

$$\psi(\vec{R}, z = \phi(\vec{R})) = 0 . \tag{7}$$

It is also a necessary condition on $\psi_i$ that it vanish at all points beneath the surface (sometimes referred to as the extinction theorem), and this has been used as a boundary condition.[2,7-9]. It has been pointed out that this so-called "extended boundary condition" may not always lead to a convergent solution; however, with Eq. (7) one is always guaranteed a solution to the problem.[10]

Garcia and Cabrera have developed a very flexible numerical method for solving the problem with the boundary conditions of Eq. (7) which has been successful in explaining elastic-scattering data.[1] The present authors have found a solution to the problem for the special case of a triangular corrugation profile which serves as an excellent check on the Garcia-Cabrera numerical method, and has also been successful in interpreting the elastic-scattering data from stepped copper surfaces.[3]

In this latter method the source function is Fourier transformed,

$$F(\vec{R}) = \sum_{N} e^{i\vec{N}\cdot\vec{R}} F_{\vec{N}} , \tag{8}$$

which casts the wave function in the form

$$\psi(\vec{r}) = e^{i\vec{K}_i\cdot\vec{R}} e^{-ik_{iz}z} - \sum_{\vec{G},\vec{N}} \frac{F_{\vec{N}} e^{i(\vec{K}_i+\vec{G})\cdot\vec{R}}}{k_{Gz}} \times \int_{uc} dR' e^{i(\vec{N}-\vec{G})\cdot\vec{R}'} e^{ik_{Gz}|z-\phi(\vec{R}')|} . \tag{9}$$

When the boundary condition of Eq. (7) is applied to the wave function in the form (9), and after subsequent Fourier transformation, the defining equation for the source function reduces to a matrix equation

$$0 = A_{\vec{M}} - \sum_{\vec{N}} F_{\vec{N}} C_{\vec{N}\vec{M}} , \tag{10}$$

where

$$A_{\vec{M}}(k_{iz}) = \int_{uc} d\vec{R} e^{-i\vec{M}\cdot\vec{R}} e^{-ik_{iz}\phi(\vec{R})} \tag{11}$$

and

$$C_{\vec{N}\vec{M}} = \sum_{\vec{G}} \frac{1}{k_{Gz}} \int_{uc} e^{i(\vec{G}-\vec{M})\cdot\vec{R}} d\vec{R} \times \int_{uc} d\vec{R}' e^{i(\vec{N}-\vec{G})\cdot\vec{R}'} e^{ik_{Gz}|\phi(\vec{R})-\phi(\vec{R}')|} . \tag{12}$$

The Fourier components of the source function $F_{\vec{N}}$ are determined by inversion of Eq. (10) and the diffraction coefficients determined from Eq. (5), which now takes the form

$$C_{\vec{G}} = \frac{1}{k_{Gz}} \sum_{\vec{N}} F_{\vec{N}} \int_{uc} d\vec{R} e^{i(\vec{N}-\vec{G})\cdot\vec{R}} e^{-ik_{Gz}\phi(\vec{R})} . \tag{13}$$

For the case of a triangular corrugation profile in one dimension all of the integrals in Eqs. (11)–(13) can be readily evaluated resulting in an essentially exact solution.

## III. THE CORRUGATED WALL OF FINITE HEIGHT

Using the same notation as for the CHW problem, we can define a finite, or "soft" corrugated-wall potential by

$$\begin{aligned} V(\vec{r}) &= 0, \quad z > \phi(\vec{R}) \\ &= V_0, \quad z < \phi(\vec{R}) . \end{aligned} \tag{14}$$

It is assumed that the energy of the incoming particle is always less than $V_0$. The exact solution of this potential is complicated by the fact that in the region of the corrugations, $\phi_{\min} < z < \phi_{\max}$, there will be both exponentially increasing and exponentially damped terms in the wave function, as well as the incoming and outgoing scattered waves of the usual CHW problem.

It is convenient to use the same integral-equation formalism as expressed in Eqs. (1) and (2), only now the integral over directions perpendicular to the surface in the transition matrix $T_{fi}$ is substantially more complicated. Thus at this point we introduce two distinct but closely related approximations. The first of these we will refer to as the Rayleigh approach since it consists of taking the correct solution for deep inside the surface, i.e.,

$$\psi(\vec{R}, z) = \sum_{\vec{N}} b_{\vec{N}} e^{i(\vec{K}_i+\vec{N})\cdot\vec{R}} e^{\kappa_n z} \tag{15}$$

with $\kappa_N^2 = 2mV/\hbar^2 - k_{Nz}^2$, and assuming this form can be extended into the selvedge region, $z \leq \phi(\vec{R})$. This is seen to be very similar in spirit to the Rayleigh method for the CHW problem, in which the form of $\psi$ valid in the asymptotic region in front of the surface is extended backwards into the selvedge region.[11]

As a second approximation we choose a slightly different form for $\psi$ inside the surface,

$$\psi(\vec{R}, z) = \sum_{\vec{N}} B_{\vec{N}} e^{i(\vec{K}_i + \vec{N})\cdot\vec{R}} e^{\kappa_N[z - \phi(\vec{R})]}, \tag{16}$$

and again assume this form can be extended into the selvedge region.

The reason for taking the two different approximations is as follows: The Rayleigh approach of Eq. (15), since it starts with an exact expression, must either lead to the correct $\psi$ according to the uniqueness theorem or it must produce no solution at all. This situation is similar to the CHW problem where the Rayleigh method is known to converge only for certain corrugations.[10,11] In the models presented below, we find that the Rayleigh approach of Eq. (15) does indeed lead to divergences, but useful results can be obtained by appropriate truncation of the problem. On the other hand, the form of Eq. (16) must lead to an approximate form for $\psi$, but the advantage of this method is that the resulting wave function is always convergent. We show below in Sec. V that the Rayleigh approach of Eq. (15) gives satisfactory results for small potential heights $V_0$, while the method using Eq. (16) is good for large $V_0$ with a substantial region of overlap in which both solutions agree.

We begin with a discussion of the solution obtained from the second assumption, Eq. (16). The transition matrix (2), which involves an integral over $z$ in the region $\phi(\vec{R}) > z > -\infty$, can be readily evaluated, giving

$$T_{fi} = V_0 \sum_{\vec{N}} B_{\vec{N}} (\kappa_N - ik_{fz})^{-1} \int d\vec{R}\, e^{i(\vec{K}_i - \vec{K}_f - \vec{N})\cdot\vec{R}} \times e^{-ik_{fz}\phi(\vec{R})}. \tag{17}$$

With the exception of the factor $V_0(\kappa_G - ik_{fz})^{-1}$, this is identical in form to the result one obtains for the CHW case using Eqs. (8) and (3). The factor $V_0(\kappa_G - ik_{fz})^{-1}$ enters the integral Eq. (1) as an extra pole, which has the effect of producing the exponentially damped waves into the surface.

Since $\phi(\vec{R})$ is periodic, the integral in (18) can be reduced to an integral over a simple unit cell with the appropriate sum over all lattice sites, which in turn can be converted to a sum over reciprocal lattice vectors

$$T_{fi} = \frac{(2\pi)^2 V_0}{a} \sum_{\vec{N}} B_{\vec{N}} (\kappa_N - ik_{fz})^{-1} \times \sum_{\vec{G}} \int_{uc} d\vec{R}\, e^{i(\vec{N} - \vec{G})\cdot\vec{R}} e^{ik_{fz}\phi(\vec{R})} \times \delta(\vec{K}_i - \vec{K}_f + \vec{G}). \tag{18}$$

Equation (18) shows explicitly that the transition matrix is nonzero only if the difference in parallel wave vector $\vec{K}_f - \vec{K}_i$ equals a reciprocal lattice vector. The sum over intermediate states in Eq. (1) can be converted in the usual manner into an integral over momentum, and, after carrying out the trivial integrations, we are left with

$$\psi_i(\vec{r}) = e^{i\vec{K}_i\cdot\vec{R}} e^{-ik_{iz}z} + \frac{mV_0}{\hbar^2 a\pi} \sum_{\vec{G}} \sum_{\vec{N}} B_{\vec{N}} e^{i(\vec{K}_i + \vec{G})\cdot\vec{R}} \times \int dq \frac{1}{(k_{Gz}^2 - q^2 + i\epsilon)(\kappa_N - iq)} \int_{uc} d\vec{R}' e^{i(\vec{N} - \vec{G})\cdot\vec{R}'} e^{iq[z - \phi(\vec{R}')]}, \tag{19}$$

where $m$ is the mass of the incident particle. The integral over $q$ can be readily carried out as a contour integration in the complex plane and the final result for the wave function in terms of the unknown constants $B_{\vec{N}}$ is

$$\psi_i(\vec{r}) = e^{i\vec{K}_i\cdot\vec{R}} e^{-ik_{iz}z} - \frac{imV_0}{\hbar^2 a} \sum_{\vec{G},\vec{N}} \frac{B_{\vec{N}} e^{i(\vec{K}_i + \vec{G})\cdot\vec{R}}}{k_{Gz}} \int_{uc} \frac{d\vec{R}' e^{i(\vec{N} - \vec{G})\cdot\vec{R}'} e^{ik_{Gz}|z - \phi(\vec{R}')|}}{(\kappa_N - ik_{Gz}\Delta)} + \frac{2mV_0}{\hbar^2 a} \sum_{\vec{G},\vec{N}} \frac{B_{\vec{N}} e^{i(\vec{K}_i + \vec{G})\cdot\vec{R}}}{(\kappa_N^2 + k_{Gz}^2)} \int_{uc} d\vec{R}' e^{i(\vec{N} - \vec{G})\cdot\vec{R}'} e^{\kappa_N[z - \phi(\vec{R}')]} S, \tag{20}$$

where the function $\Delta$ is +1 if $(z - \phi) > 0$ and is −1 if $(z - \phi) \leq 0$, while $S = 0$ if $(z - \phi) > 0$ and equals +1 if $(z - \phi) \leq 0$. A comparison with Eq. (9) shows that the first two terms on the right-hand side of (20) are very similar to the hard-wall case, while the last term is nonvanishing only inside the surface and is a sum of exponentially damped waves. In particular we note that the factor $e^{ik_{Gz}|z - \phi(\vec{R})|}$ ensures that in the selvedge region the wave function will contain both incoming and outgoing scattered waves, and for $z < \phi(R)$ gives a sum of differential waves.

From the form of (20) in the asymptotic region in front of the surface, $z > \phi_{max}$, it is seen that the coef-

ficients of the diffracted beams are

$$C_{\vec{G}}=\frac{-imV_0}{\hbar^2 a}\frac{1}{k_{Gz}}\sum_{\vec{N}}\frac{B_{\vec{N}}}{(\kappa_N-ik_{Gz})}\int_{uc}d\vec{R}\,e^{i(\vec{N}-\vec{G})\cdot\vec{R}}e^{-ik_{Gz}\phi(\vec{R})} \tag{21}$$

with the diffracted intensities given by (6). Again this is very similar in form to the corresponding coefficient for the hard-wall problem given in Eq. (13).

The final problem is the determination of the coefficients $B_{\vec{N}}$, and for this we use the boundary condition implied by Eq. (16) at the surface $z=\phi(\vec{R})$,

$$\psi_i(\vec{R},z=\phi(\vec{R}))=\sum_{\vec{N}}B_{\vec{N}}e^{i(\vec{K}_i+\vec{N})\cdot\vec{R}}. \tag{22}$$

Evaluating the wave function (20) at the surface together with condition (22) gives the defining equation for the $B_{\vec{N}}$:

$$\sum_N B_{\vec{N}}e^{i\vec{N}\cdot\vec{R}}=e^{-ik_{iz}\phi(\vec{R})}-\frac{imV_0}{\hbar^2 a}\sum_{\vec{G},\vec{N}}\frac{B_{\vec{N}}e^{i\vec{G}\cdot\vec{R}}}{k_{Gz}}\int_{uc}\frac{d\vec{R}\,e^{i(\vec{N}-\vec{G})\cdot\vec{R}'}e^{ik_{Gz}|\phi(R)-\phi(\vec{R}')|}}{(\kappa_N-ik_{Gz}\Delta)}$$
$$+\frac{2mV_0}{\hbar^2 a}\sum_{\vec{G},\vec{N}}\frac{B_N e^{i\vec{G}\cdot\vec{R}}}{(\kappa_N^2+k_{Gz}^2)}\int_{uc}d\vec{R}'\,e^{i(\vec{N}-\vec{G})\cdot\vec{R}'}e^{\kappa_N[\phi(\vec{R})-\phi(\vec{R}')]}S, \tag{23}$$

where the argument of both $\Delta$ and $S$ is $\phi(\vec{R})-\phi(\vec{R}')$. Fourier transforming both sides of (22) leads to a matrix equation

$$aB_{\vec{M}}=A_{\vec{M}}+\sum_{\vec{N}}B_{\vec{N}}H_{\vec{N}\vec{M}}+\sum_{\vec{N}}B_{\vec{N}}D_{\vec{N}\vec{M}}, \tag{24}$$

where $A_{\vec{M}}$ is defined by (11),

$$H_{NM}=-\frac{imV_0}{\hbar^2 a}\sum_{\vec{G}}\frac{1}{k_{Gz}}\int_{uc}d\vec{R}\,e^{i(\vec{G}-\vec{M})\cdot\vec{R}}\int_{uc}d\vec{R}'\,\frac{e^{i(\vec{N}-\vec{G})\cdot\vec{R}'}e^{ik_{Gz}|\phi(\vec{R})-\phi(\vec{R}')|}}{(\kappa_N-ik_{Gz}\Delta)} \tag{25}$$

and

$$D_{\vec{N}\vec{M}}=\frac{2mV_0}{\hbar^2 a}\sum_{\vec{G}}\frac{1}{(\kappa_N^2+k_{Gz}^2)}\int_{uc}d\vec{R}\,e^{i(\vec{G}-\vec{M})\cdot\vec{R}}\int_{uc}d\vec{R}'e^{i(\vec{N}-\vec{G})\cdot\vec{R}'}e^{\kappa_N[\phi(\vec{R})-\phi(\vec{R}')]}S. \tag{26}$$

Again we see the similarities between the present soft-wall calculation and the corresponding hard-wall case shown in Eq. (10). The nonvanishing term on the left-hand side of (24) arises from the difference in boundary conditions (i.e., the wave function does not vanish at the surface), while the final term on the right-hand side is the contribution from the penetration of the wave function into the surface.

At this point, before carrying out calculations for a specific model, it is interesting to consider the two special limits, the hard-wall case $V_0\to\infty$ and the specular scattering limit for a flat surface, $\phi(\vec{R})=$ constant.

In the limit $V_0\to\infty$ we note that the matrix $H_{\vec{N}\vec{M}}$ of Eq. (23) becomes

$$H_{\vec{N}\vec{M}}\xrightarrow[V_0\to\infty]{}-\frac{i(mV_0)^{1/2}}{\sqrt{2}}\frac{1}{\hbar a}C_{\vec{N}\vec{M}}, \tag{27}$$

where $C_{\vec{N}\vec{M}}$ is defined by (12), and the matrix $D_{\vec{N}\vec{M}}$ is given by

$$D_{\vec{N}\vec{M}}\xrightarrow[V_0\to\infty]{}\frac{1}{a}D'_{\vec{N}\vec{M}}, \tag{28}$$

where $D'_{\vec{N}\vec{M}}$ is just the double integral of (26) and is clearly a decreasing function of $V_0$ due to the decaying exponential in the integral. Thus the matrix equation (24) becomes

$$A_{\vec{M}}=\sum_{\vec{N}}B_{\vec{N}}\,(i(mV_0/2)^{1/2}/\hbar a)C_{\vec{N}\vec{M}}-\frac{1}{a}D'_{\vec{N}\vec{M}}+a\delta_{\vec{N}\vec{M}}. \tag{29}$$

Clearly in the limit $V_0\to\infty$ the only important term in the parentheses on the right is the one proportional to $\sqrt{V_0}$; thus the coefficients $B_N$ are given by

$$A_{\vec{M}}=\sum_{\vec{N}}(i(mV_0/2)^{1/2}/\hbar a)B_{\vec{N}}C_{\vec{N}\vec{M}}. \tag{30}$$

In the same limit the diffraction coefficients of Eq. (20) are given by

$$C_{\vec{G}}=-i((mV_0/2)^{1/2}/\hbar a)$$
$$\times\sum_{\vec{N}}B_{\vec{N}}\int_{uc}d\vec{R}\,e^{i(\vec{N}-\vec{G})\cdot\vec{R}}e^{-ik_{Gz}\phi(\vec{R})} \tag{31}$$

upon making the association $[(mV_0)^{1/2}/2](i/\hbar a)B_{\vec{N}}=F_{\vec{N}}$, Eqs. (30) and (31) are seen to be identical

to (10) and (13), respectively, which demonstrates that this function has the correct hard-wall limit.

Finally we show that the problem reduces to the correct result having scattered beam of unit intensity for a flat surface. Setting $\phi(\vec{R}) = b$, where $b$ is a constant we can readily evaluate all the terms appearing in Eq. (24). From Eq. (11) we have

$$A_{\vec{M}} = e^{-ik_{iz}b}\int_{uc} d\vec{R}\, e^{-i\vec{M}\cdot\vec{R}} = a\, e^{-ik_{iz}b}\delta_{\vec{M},0}. \tag{32}$$

The double integrals appearing in the matrices $H_{\vec{N}\vec{M}}$ and $D_{\vec{N}\vec{M}}$ also reduce to $\delta$ functions. From Eq. (25) we have

$$H_{\vec{N}\vec{M}} = \frac{-imV_0 a}{\hbar^2}\frac{1}{k_{Nz}}\frac{1}{(\kappa_N + ik_{Nz})}\delta_{\vec{N},\vec{M}}, \tag{33}$$

and Eq. (26) gives

$$D_{\vec{N}\vec{M}} = a\delta_{\vec{N},\vec{M}}. \tag{34}$$

Equation (24) for the coefficients $B_{\vec{N}}$ becomes

$$aB_{\vec{M}} = a\, e^{-ik_{iz}b}\delta_{\vec{M},0} - \frac{imV_0 a}{\hbar^2}\frac{1}{k_{Mz}}\frac{1}{\kappa_M + ik_{Mz}}B_{\vec{M}} + aB_{\vec{M}}. \tag{35}$$

We see that the term on the right arising from the nonzero boundary condition exactly cancels the term on the far left-hand side, arising from the penetration of the wave. The $B_m$ matrix has only one nonvanishing component,

$$B_{\vec{M}} = \frac{-i\hbar^2 k_{Mz}(\kappa_M + ik_{Mz})\, e^{ik_{iz}b}}{mV_0}\delta_{\vec{M},0}. \tag{36}$$

The integral in the expression for the diffracted beam coefficients, Eq. (21), is also trivial, and we obtain

$$C_{\vec{G}} = -\frac{(\kappa_G + ik_{Gz})}{(\kappa_G - ik_{Gz})}\delta_{\vec{G},0}. \tag{37}$$

It is clear from Eq. (6) that the above result gives only a specularly scattered beam of unit intensity.

A consideration of the Rayleigh approach starting from Eq. (15) leads to results very similar to those contained above in Eqs. (20)–(26); however, there are some important differences. Again the integral over directions perpendicular to the surface in the transition matrix (2) can be readily evaluated giving

$$T_{fi} = V_0\sum_{\vec{N}} b_{\vec{N}}(\kappa_N - ik_{fz})^{-1} \times\int d\vec{R}\, e^{i(\vec{K}_i - \vec{K}_f + \vec{N})\cdot\vec{R}}\, e^{(\kappa_N - ik_{zf})\phi(\vec{R})}. \tag{38}$$

The difference with the previous Eq. (17) is the additional term $\kappa_N\phi(\vec{R})$ in the argument of the exponential. Again making use of the periodicity of the potential, many of the integrals of Eq. (1) can be evaluated, leading to the form for the wave function corresponding to Eq. (20):

$$\psi_i(\vec{r}) = e^{i\vec{K}_i\cdot\vec{R}}e^{-ik_{iz}z} + \frac{mV_0}{\hbar^2 a}\sum_{\vec{G},\vec{N}}\frac{b_{\vec{N}}\, e^{i(\vec{K}_i + \vec{G})\cdot\vec{R}}}{k_{Gz}}\int_{uc}\frac{dR'\, e^{i(\vec{N}-\vec{G})\cdot\vec{R}'}\, e^{\kappa_N\phi(\vec{R}')}\, e^{ik_{Gz}|z-\phi(\vec{R}')|}}{k_{Gz}\Delta + i\kappa_N} + \frac{2mV_0}{\hbar^2 a}\sum_{\vec{G},\vec{N}}\frac{b_{\vec{N}}\, e^{i(\vec{K}_i + \vec{G})\cdot\vec{R}}}{(\kappa_N^2 + k_{Gz}^2)}\int_{uc} d\vec{R}'\, e^{i(\vec{N}-\vec{G})\cdot\vec{R}'}e^{\kappa_N z}S, \tag{39}$$

where the functions $S$ and $\Delta$ are defined following Eq. (20). The boundary conditions implied by Eq. (15) are

$$\psi(\vec{R}, \phi(\vec{R})) = \sum_N b_{\vec{N}}\, e^{i(\vec{K}_i + \vec{N})\cdot\vec{R}}\, e^{\kappa_N\phi(\vec{R})}. \tag{40}$$

When this condition is impressed upon the wave function (39), and, after subsequent Fourier transformation in directions parallel to the surface, we arrive at the following matrix equation for $b_N$ corresponding to Eq. (24):

$$\sum_{\vec{N}} b_{\vec{N}} f_{\vec{N}\vec{M}} = A_{\vec{M}} + \sum_{\vec{N}} b_{\vec{N}}(h_{\vec{N}\vec{M}} + d_{NM}), \tag{41}$$

where

$$f_{\vec{N}\vec{M}} = \int_{uc} d\vec{R}\, e^{i(\vec{N}-\vec{M})\cdot\vec{R}}\, e^{\kappa_N\phi(\vec{R})} = A_{\vec{M}-\vec{N}}(i\kappa_N). \tag{42}$$

The element $h_{\vec{N}\vec{M}}$ is identical to $H_{\vec{N}\vec{M}}$ of Eq. (25), except for an additional factor of $e^{\kappa_N\phi(\vec{R}')}$ in the integrand of the first integral, and $d_{\vec{N}\vec{M}}$ is identical to $D_{\vec{N}\vec{M}}$ of Eq. (25), except that the factor $e^{-\kappa_N\phi(\vec{R}')}$ is missing from the integrand.

A comparison of the two different approaches to the problem shows that the final forms of the wave functions differ only by the presence or absence of factors of $e^{\kappa_N\phi(\vec{R})}$. However, from the point of view of convergence arguments, these small differences are of extreme importance. If we attempt to examine the hard-wall limit ($V_0 \to \infty$) of Eq. (39), we find that, since $\kappa_N \to \sqrt{V_0}$, the extra factors of $e^{\kappa_N\phi(\vec{R})}$ become very large or very small according to the sign of $\phi(\vec{R})$. In fact, the hard-wall limit for the Rayleigh approach does not in general exist, and this is verified by the numerical calculations presented below. On the other hand, the specular

limit for $\kappa \to$ constant is readily obtained for $\psi_i(\vec{r})$ of Eq. (39) for any finite value of $V_0$.

## IV. CALCULATIONS FOR THE TRIANGULAR SURFACE CORRUGATION

In order to obtain numerical results for a physical system, we have carried out calculations for both of the approximations outlined above using a one-dimensional triangular surface corrugation profile. This seems to be a reasonable model for describing the scattering data from stepped metal surfaces.[3,12]

If $x$ is taken to be the axis in the surface plane perpendicular to the corrugations, the triangular profile is defined by

$$\phi(x) = -2hax/b, \quad 0 \le x \le b$$
$$= -2ha(a-x)/(a-b), \quad b \le x \le a, \tag{43}$$

where, as shown in Fig. 1, $a$ is the period, $b$ is the vertex position, and $2ha$ is the total trough-to-crest amplitude. With this corrugation all of the Fourier integrals involved in obtaining the two different wave functions can now be obtained analytically, and the only remaining calculation is the resolution of the two systems of linear Eqs. (24) and (41) to obtain the unknown coefficients, a relatively simple numerical procedure.

Taking the same order as in Sec. III, we will consider first the solution arising from the approximation of Eq. (16). In this one-dimensional model the reciprocal lattice vectors such as $\vec{G}$ become $G = (2\pi/a)g$ $(g = 0, \pm 1, \pm 2, \ldots)$ and Eq. (24) for the $B_{\vec{N}}$ coefficients becomes

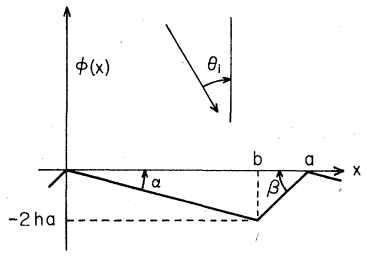


FIG. 1. The triangular corrugation profile as defined by Eq. (43).

$$0 = A_M + \sum_N B_N (H_{NM} + D_{NM} - a\delta_{NM}). \tag{44}$$

The explicit form for the various matrices in (44) is as follows:

$$A_M(k_{iz}) = \frac{2k_{iz}ha^2[e^{-i(Mb-2k_{iz}ha)}-1]}{i(Mb-2k_{iz}ha)[M(a-b)+2k_{iz}ha]}, \tag{45}$$

$$H_{NM} = -\frac{imV_0}{\hbar^2}\sum_G Q_{NM}(G), \tag{46}$$

where if $N \neq M$

$$Q_{NM}(G) = 2h\left[(e^{i(N-M)b}-1)\left(\frac{\beta-\delta}{N-M} + \frac{(a-b)\beta}{(M+G)a+(N-M)b} + \frac{b\delta}{(N-M)b-(N+G)a}\right)\right.$$
$$\left. - \alpha(e^{i(N-M)b} - e^{i[(N+G)b-2k_{Gz}ha]}) - \gamma(e^{-i[(M+G)b+2k_{Gz}ha]}-1)\right], \tag{47}$$

where

$$\beta(b) = \frac{2hab\kappa_N - ib^2(N+G)}{ha[(N+G)^2b^2 - (2k_{Gz}ha)^2](k_{Gz}^2+\kappa_N^2)}, \tag{48}$$

$$\delta(b) = \beta^*(a-b), \tag{49}$$

$$\alpha(b) = \frac{-2k_{Gz}ha^3}{[(N+G)(a-b)+2k_{Gz}ha][(N+G)b-2k_{Gz}ha][(M+G)b-2k_{Gz}ha][(M+G)(a-b)+2k_{Gz}ha](-ik_{Gz}+\kappa_N)}, \tag{50}$$

$$\gamma(b) = \alpha^*(a-b). \tag{51}$$

Special care must be taken when $b/a$ approaches a rational number to use the correct limiting forms for $Q_{NM}(G)$. The explicit forms for the other matrices appearing in Eq. (44) are similar. The reflection coefficients of Eq. (21) are given by

$$C_G = \frac{mV}{\hbar^2 a}\frac{1}{k_{Gz}}\sum_N \frac{B_N}{(\kappa_N - ik_{Gz})}A_{G-N}(k_{Gz}), \tag{52}$$

where $A_{G-N}(k_{Gz})$ is given by (45), with $M$ replaced by $G-M$ and $k_{iz}$ replaced by $k_{Gz}$.

The detailed expressions for the Rayleigh approach are also quite similar to the above. Since they are straightforward but somewhat lengthy, we need not present them here.

## V. RESULTS AND DISCUSSION

We have carried out extensive numerical calcula-

tions for both of the approaches outlined above. Once again we will discuss first the approximate solution arising from assumption (16) and then consider the Rayleigh approach afterwards.

To obtain the numerical results we convert the infinite system of Eq. (44) into a finite matrix equation by truncation at a dimension large enough to ensure good convergence. The internal summations over $G$ such as in Eq. (46) are carried out over a sufficient number of terms to obtain the desired accuracy of the respective matrix elements. Equation (44) is inverted to obtain $B_N$ and then the diffraction coefficients and intensities are calculated from (52) and (6).

We find that the method gives good results for a large range of the parameters $a$, $b$, $h$, and $V_0$. (By "good results" we mean that the individual diffracted intensities are stable and the sum of all intensities, i.e., the unitarity, is very nearly one.) Furthermore, we find that the solution is always convergent for any values of the above parameters, that is to say, that the calculated diffracted intensities stabilize and remain stable as the matrix of Eq. (44) is truncated at larger and larger values. This convergence is in fact guaranteed since the matrices of Eq. (44) are of the same general form as those which have been discussed elsewhere for the corresponding CHW problem.[10]

Since this is an approximate solution to the problem, we do not expect the unitarity to be exactly one, but it should be very near unity if the solution is to be considered good. The quality of the solution is most sensitive to the parameters $h$ and $V_0$. However, for values of $V_0$ around five times the incident energy and for $h$ of the order 0.1 or less, we find that the unitarity typically differs from one by no more than 1 or 2%. We find that the dimension at which the matrix equation is truncated should be larger than the number of real diffracted beams, but still of that same order of magnitude. Best results are obtained if the sum over $G$ in (25) and (26) contains at least as many terms as the dimension of the truncated matrix. We obtain results for all angles of the incident beam, and the convergence seems to improve as the angle of incidence is increased away from the normal. For large values of $V_0$ ($\gtrsim$ten times the incident energy), the results approach very closely those of the exact hard-wall calculation. For small $V_0$ the approximation fails, although we find that the unitarity remains good in many instances even for $V_0$ as small as two or three times the incident energy.

Shown in Table I are the results of calculations for the scattering of helium using a set of parameters exhibiting only seven diffracted beams, together with a comparison with the exact hard-wall solution. For all the calculations $a = 3\times10^{8}$ cm, $b = 0.75a$, $h = 0.1$, and the incident wave vector is $7.06\times10^{8}$ cm$^{-1}$. The incident beam makes an angle of 60° with the surface in the manner shown in Fig. 1. Results are obtained which are unitary to within 1% for potential heights as low as three times the incident energy.

It is obvious from the table that there is little difference between the CHW results and the present calculations for $V_0 = 100E_i$ or greater. This is not surprising in view of the fact that the penetration depths $1/\kappa_N$ are of the order $2\times10^{-10}$ cm or less, while the incident wavelength is $8.9\times10^{-9}$ cm. However, for $V_0$ of the order $10\,E_i$ or less, the differences become much more pronounced. For the case $V_0 = 3E_i$ ($1/\kappa_N \leq 1.0\times10^{-9}$ cm) the specular beam is enhanced by nearly 20% while the rainbow associated with the third-order diffracted peak has disappeared. The effect of wave penetration into the surface tends to destroy the well-defined rainbow pattern and push all of

TABLE I. Diffraction intensities for helium incident on a triangular profile for several values of $V_0$ using the approximation of Eq. (16). The beam is incident at an angle of 60° as shown in Fig. 1. $a = 3$ Å, $b = 0.75a$, and the magnitude of the incident wave vector is $7.26\times10^{8}$ cm$^{-1}$. $\kappa$ is the smallest value of $\kappa_N$ and corresponds to order 3 in this case.

| Order | Scattered angle | $V_0 = 100E_i$ | $V_0 = 10E_i$ | $V_0 = 5E_i$ | $V_0 = 3E_i$ | CHW $V_0 = \infty$ |
|---|---|---|---|---|---|---|
| 0 | 60.0° | 0.315 | 0.331 | 0.349 | 0.367 | 0.314 |
| 1 | 34.7° | 0.144 | 0.150 | 0.153 | 0.153 | 0.143 |
| 2 | 15.8° | 0.155 | 0.157 | 0.156 | 0.149 | 0.154 |
| 3 | − 1.4° | 0.174 | 0.172 | 0.166 | 0.153 | 0.173 |
| 4 | −18.8° | 0.149 | 0.142 | 0.134 | 0.122 | 0.148 |
| 5 | −38.1° | 0.060 | 0.052 | 0.047 | 0.041 | 0.060 |
| 6 | −66.0° | 0.007 | 0.006 | 0.005 | 0.004 | 0.006 |
| Unitarity | | 1.004 | 1.009 | 1.009 | 0.989 | 1.000 |
| $1/\kappa$ | | $1.42\times10^{-10}$ cm | $4.12\times10^{-10}$ cm | $7.08\times10^{-10}$ cm | $1.00\times10^{-9}$ cm | 0.0 |

the intensities toward the specular. In a very crude sense, one would expect the potential strength $V_0$ to correspond roughly to the energy necessary to make an atom penetrate substantially into the surface, which for the case of He at a metal surface would lead to a ratio of $V_0/E \sim 10$ or higher. However, in the surface-scattering problem the slope of the potential may be much more important than the total height in determining the wave penetration. Hence it is quite possible that the true experimental situation allows wave-function penetration corresponding to the larger values of $1/\kappa_N$ calculated with this model. In this case one may expect the experimental results to differ significantly from the results of a CHW calculation.

Perhaps a much better test of the true importance of the wave penetration is that shown in Table II. This shows calculations for the triangular corrugation profile which has been used to interpret the experimental data of Lapujoulade and Lejay for the scattering of helium from stepped copper surfaces.[12] The experiments were carried out using the (117) face of copper which consists of (100) terraces separated by linear steps parallel to the [110] direction. The period is 9.13 Å, and the small angle $\alpha$ shown in Fig. 1 [the angle between the plane of a (117) surface and the (100) terraces] is 11.25°. $\beta$ (the angle of the step faces) is chosen to be 20°, the value which gives the best fit with the experimental data for the hard-wall calculation.[3] This corresponds to a value of $h = 0.065$. The angle of incidence if 60°. For this experimental configuration there are 32 open channels for diffracted beams; however, we have shown in Table II only the ones which have non-negligible intensities, and all of these are scattered on the opposite side of the surface normal from the incident beam.

It is evident that the present soft-wall calculations give results with good unitarity for potential heights as small as three-times the incident energy. The most striking thing about the data in Table II is the fact that the effect of wave penetration into the surface does not affect the overall picture of the scattered intensities very much. The biggest change is in the diffracted peak of order 2, which nearly coincides with the classical rainbow angle for forward scattering from the broad (100) terraces. This rainbow peak is reduced by about 15% from the CHW calculation if the potential height is lowered to $3E_i$. On the other hand, the rainbow pattern associated with diffracted orders 7, 8, and 9 is enhanced slightly. Thus, even though it appears that the penetration of the wave function tends to reduce the rainbow patterns, this is certainly not always the case.

Turning now to the Rayleigh approach, the truncation and resolution of the system of Eqs. (41) and subsequent calculations of the diffracted intensities follows the same lines as outlined above. We have found, not unexpectedly, that this approach suffers from numerical convergence problems which are quite similar to those that have been

TABLE II. Comparison with the experimental results of Lapujoulade and Lejay for various values of $V_0$ using the approximation of Eq. (16). The incident wave vector is $1.1\times10^9$ cm$^{-1}$, $\theta_i = 60°$, and the triangular profile is defined by $a = 9.13$ Å, $\alpha = 11.25°$, and $\beta = 20°$.

| Order | Scattering angle | $V_0 = 100E_i$ | $V_0 = 10E_i$ | $V_0 = 5E_i$ | $V_0 = 3E_i$ | CHW $V = \infty$ | Experiment |
|---|---|---|---|---|---|---|---|
| 2 | 82.4° | 0.239 | 0.233 | 0.225 | 0.213 | 0.240 | 0.141 ± 20 |
| 1 | 68.2° | 0.007 | 0.007 | 0.007 | 0.006 | 0.007 | 0.000 ± 5 |
| 0 | 60.0° | 0.019 | 0.019 | 0.019 | 0.019 | 0.019 | 0.009 ± 2 |
| −1 | 53.5° | 0.040 | 0.040 | 0.040 | 0.039 | 0.040 | 0.022 ± 5 |
| −2 | 47.8° | 0.057 | 0.058 | 0.058 | 0.058 | 0.057 | 0.025 ± 10 |
| −3 | 42.7° | 0.053 | 0.053 | 0.054 | 0.053 | 0.053 | 0.030 ± 10 |
| −4 | 38.0° | 0.021 | 0.022 | 0.022 | 0.021 | 0.021 | 0.000 ± 20 |
| −5 | 33.6° | 0.000 | 0.000 | 0.000 | 0.000 | 0.000 | 0.000 ± 20 |
| −6 | 29.4° | 0.042 | 0.043 | 0.043 | 0.043 | 0.041 | 0.057 ± 20 |
| −7 | 25.4° | 0.134 | 0.138 | 0.139 | 0.138 | 0.132 | 0.089 ± 30 |
| −8 | 21.4° | 0.188 | 0.193 | 0.195 | 0.193 | 0.185 | 0.063 ± 40 |
| −9 | 17.6° | 0.142 | 0.146 | 0.147 | 0.145 | 0.140 | 0.079 ± 40 |
| −10 | 13.9° | 0.051 | 0.053 | 0.053 | 0.052 | 0.051 | 0.053 ± 50 |
| −11 | 10.2° | 0.004 | 0.004 | 0.004 | 0.004 | 0.004 | 0.000 ± 50 |
| −12 | 6.6° | 0.002 | 0.002 | 0.002 | 0.002 | 0.002 | 0.000 ± 60 |
| −13 | 3.0° | 0.004 | 0.004 | 0.004 | 0.004 | 0.004 | 0.000 ± 60 |
| −14 | 0.6° | 0.000 | 0.000 | 0.000 | 0.000 | 0.000 | 0.000 ± 70 |
| Unitarity | | 1.006 | 1.015 | 1.014 | 0.995 | 0.998 | 0.568 |

TABLE III. Comparison of the approximation of Eq. (16) with the Rayleigh approach for the same system as described in Table I.

| Order | Corrugated hard wall | Approximate soft-wall $V_0 = 3E_i$ | Rayleigh approach $V_0 = 3E_i$ | Rayleigh approach $V_0 = 1.1E_i$ |
|---|---|---|---|---|
| 0 | 0.314 | 0.367 | 0.332 | 0.333 |
| 1 | 0.143 | 0.153 | 0.147 | 0.151 |
| 2 | 0.154 | 0.149 | 0.149 | 0.149 |
| 3 | 0.173 | 0.153 | 0.161 | 0.151 |
| 4 | 0.148 | 0.122 | 0.132 | 0.132 |
| 5 | 0.060 | 0.041 | 0.050 | 0.060 |
| 6 | 0.006 | 0.004 | 0.008 | 0.011 |
| Unitarity | 1.000 | 0.989 | 0.980 | 0.989 |

often noticed when the Rayleigh method or other similar simple methods are used in the CHW problem.[10] If the size of the system of Eqs. (41) is truncated at a value not too much greater than the number of allowed diffraction channels, then good results can often be obtained. If the size of the system is increased, eventually the solution becomes unstable, and the unitarity is lost, rather like the behavior of an asymptotic expansion.

We find that, within the constraints of proper truncation, the solution becomes better and better with smaller $V_0$, exactly contrary to the other approximation discussed here. On the other hand, the results become poor for large $V_0$, reflecting the fact that this method does not give the correct CHW limit as $V \to \infty$.

Shown in Table III are the results of some selected calculations for the same system as in Table I. The results of the two different approaches for the same potential strength $V_0$ are very nearly the same. The Rayleigh approach does not work with this system for $V_0$ much greater than three times the incident energy, but for the small value $V_0 = 1.1E_i$ the unitarity is quite good and the intensities of the diffracted beams are still not appreciably different from the CHW values. Thus it appears that, in spite of its convergence difficulties, the Rayleigh approach works well in precisely the same region where the other approximation fails, but there is an overlap region in which both solutions give practically identical results.

A number of interesting conclusions can be drawn from this work. We have shown that with a simple approximation one can obtain solutions for the finite corrugated wall which work well for a variety of systems. Basically, the approximations amount to solving the integral form for the Schrödinger equation by using a limited amount of known information about the exact solution. In this case, the exact asymptotic form of the solution inside the surface is known, and we make the assumption that such a form can be extended into the selvedge region.

This work also answers a number of questions concerning the effects of allowing the wave function to penetrate into the surface. One can argue that a disadvantage of the CHW model is that it forces the wave function to vanish at the surface, but it is the very region of overlap of the wave function with the surface which is where the interaction should be most important. However, the wave function goes to zero at the surface, but the potential rises to infinity in such a manner that their product is nonzero, as shown by Eq. (3). It seems that this overlap, which appears only at the surface, is a sufficient approximation to account reasonably well for the largest part of the true penetration of the wave into the surface. The main effect of softening the potential is a tendency to destroy or reduce the quantum-mechanical rainbow pattern; however, this effect is not strong even under conditions in which the wave function can penetrate a wavelength or more into the surface. Nevertheless, we have shown in these calculations that the penetration of the wave function can easily give corrections of 15–20%. Thus, eventually it appears that a correction for this effect will be necessary in a complete theory of atom-surface scattering.

Finally, we would like to mention that this work, although written from the point of view of the atom-surface scattering problem, is valid for the reflection of all scalar waves under conditions in which damped penetration of the wave can occur. The methods can also be readily extended to the problem of scattering of vector waves.

## ACKNOWLEDGMENTS

We would like to thank Dr. C. Manus, Dr. D. Degras, and particularly Dr. J. Lapujoulade for helpful discussions and encouragement during the course of this work.

*The work of J. R. Manson was carried out while the author was a visiting scientist at the Centre d'Etudes Nucléaires de Saclay, Service de Physique Atomique, B. P. 2, 91190 Gif-sur-Yvette, France.

[1]N. Garcia and N. Cabrera, in *Proceedings of the 7th International Vacuum Congress and 3rd International Conference on Solid Surfaces, Vienna*, 1977, edited by R. Dobrozemsky, F. Rudenauer, F. P. Viehböck, and A. Breth, R. Dobrozemsky *et al.*, Vienna, 1977), p. 379; N. Garcia, Phys. Rev. Lett. 37, 912 (1976); N. Garcia, and N. Cabrera, Phys. Rev. B 18, 576 (1978).

[2]R. I. Masel, R. P. Merrill, and W. H. Miller, Phys. Rev. B 12, 5545 (1975).

[3]G. Armand and J. R. Manson, Phys. Rev. B 18, 6510 (1978).

[4]G. Armand, J. Lapujoulade, and J. R. Manson, Surf. Sci. 82, L625 (1979).

[5]C. E. Harvie and J. H. Weare, Phys. Rev. Lett. 40, 187 (1978).

[6]N. Garcia, Frank O. Goodman, V. Celli, and N. R. Hill (unpublished).

[7]John A. DeSanto, J. Acoust. Soc. Am. 57, 1195 (1975).

[8]P.C. Waterman, J. Acoust. Soc. Am. 57, 791 (1975).

[9]F. O. Goodman, J. Chem. Phys. 66, 976 (1977).

[10]G. Armand and J. R. Manson, Phys. Rev. B 19, 4091 (1979).

[11]For a discussion of the range of validity of the Rayleigh method see R. F. Miller, Radio Sci. 8, 785 (1973).

[12]J. Lapujoulade and Y. Lejay, Surf. Sci. 69, 354 (1977).